A Transient Dynamic Analysis of Mechanical Seals Including Asperity Contact and Face Deformation©

ITZHAK GREEN (Fellow, STLE)
Georgia Institute of Technology
George W. Woodruff School of Mechanical Engineering
Atlanta, Georgia 30332-0405

Face seals are typically designed to be in contact at standstill. However, as speed and pressure build up, the seal faces deform from their factory flat conditions because of viscous and dry friction heating, as well as mechanical and centrifugal effects. It is imperative that such deformations form a converging gap for radial flow to ensure stable operation and to promote favorable

dynamic tracking between stator and rotor. A numerical simulation is presented for the transient response of a face seal that is subjected to forcing misalignments while speeds and pressures are ramped up and down. Asperity contact forces and transient face deformation caused by viscous heating are included. A new closed-form solution is obtained for the elastoplastic contact model, which allows seamless transition between contacting and noncontacting modes of operation. The model is then used to calculate face contact forces that occur predominantly during start-up and shutdown. The viscous heating model shows that the time-dependent deformation (coning) is hereditary and that it lags behind the instantaneous heat generation. The dynamic analysis

NOMENCLATURE

B = balance ratio

C = centerline clearance, C_o+Z

C_o = design clearance

D_z = axial damping coefficient

D = angular damping coefficient

E = equivalent modulus of elasticity, $\left(\frac{1-\nu_1^2}{E_1} + \frac{1-\nu_2^2}{E_2}\right)^{-1}$

F = force

h = local film thickness

H = hardness of the softer material

I = transverse moment of inertia, $m \cdot r_g^2/2$

K_z = axial stiffness coefficient

K = angular stiffness coefficient

M = moment

M_{Xi} = moment due to stator initial misalignment

m = stator mass

p = pressure

Q^* = flow

Q = normalized flow, $\frac{Q^*}{\pi(p_i-p_o)C_o^3/6\mu}$

r = radial coordinate

t = time

Z = axial degree of freedom

β = face coning

γ = relative misalignment

γ_o = relative misalignment caused by rotor runout alone

γ_r = rotor runout

γ_s = stator nutation

γ_{si} = stator initial misalignment

γ_{sl} = steady-state stator response due to γ_{si} alone

γ_{sr} = steady-state stator response due to γ_r alone

θ = angular coordinate

μ = viscosity

ν = Poisson's ratio

σ = surface heights composite standard deviation

τ = thermal time constant

ψ = precession

ω = shaft angular velocity at steady-state

Subscripts

c = contact

cls = closing force

f = fluid film

g = gyration radius

hyd = hydraulic force

i = inner radius

o = outer radius

r = rotor

ref = reference value

s = stator, or flexible support

spr = spring closing force

provides a numerical solution for the seal motion in axial and angular modes. The eventual build up of hydrostatic pressure and coning during startup generates opening forces and moments that separate the seal faces, resulting in noncontacting operation. The reverse occurs during shutdown; however, because of the thermal time constant a seal may continue to leak even after it returns to standstill. The analysis and simulation results compare very well with a closed-form solution that predicts a critical speed of separation of contacting seals.

KEY WORDS

Mechanical Seals; Face Seals; Transient; Dynamics; Contacting; Noncontacting; Asperity Contact; Coning; Face Deformation

INTRODUCTION

Mechanical face seals are lapped flat when new. However, changes in operating conditions, particularly during startup and shutdown, inevitably cause the faces to deform from their initial flat state. Such deformations are caused in part by viscous heating, pressure, centrifugal effects, etc. (Doust and Parmar, 1986; Ruan et al., 1997). It has well been established that face coning has a paramount effect on seal dynamics (e.g., Green and Etsion, 1985, 1986; Green and Barnsby, 2001). Such dynamics determines the relative position between stator and rotor which in turn directly affects viscous (and perhaps frictional) heating. Hence, all of the aforementioned effects are entangled. It is, therefore, necessary to solve the dynamics and face deformation in one coupled system when transients are concerned.

Quasi-static transient analyses of face seals have been performed by Parmar (1992), and Harp and Salant (1997) who assumed perfect alignment (axisymmetric conditions), stable operation, displacement in the axial mode only, and no inertia terms (i.e., dynamics has not been considered). Parmar (1992) included a finite element code to calculate deformations within an iterative procedure, where others used an influence coefficients technique similar to that formulated by Taylor (1992), and Ruan et al. (1997). However, in practical seals manufacturing tolerances, assembly imperfections, and field conditions (e.g., bent shafts, gravity) impose upon the rotor and stator misalignments that force the system in the angular mode. Green and Etsion (1985, 1986) have demonstrated that the axial mode of motion is actually quite benign, and even if a seal is stable in the axial mode it may be unstable in the angular mode. Furthermore, the coupling that exists between axial and angular modes prevents the idealization of a single degree of freedom (or axisymmetric) analysis for practical seals. Likewise, the technique of time invariant influence coefficients is useful only for quasi-static processes. In real seals undergoing transients, thermal inertia is bound to create a lag between cause and event, i.e., there is a lag between the instant of viscous heating and face deformation. In other words the seal behavior is hereditary.

The works by Green and Etsion (1986) and Green and Barnsby (2001), do solve the coupled problem of axial and angular modes, and are capable of solving for stability, steady-state, and transient responses. However, they have not included contact mechanics or time dependent deformation, as these analyses consider noncontacting operation only. It is the intent of this work to rectify this problem. While the technique presented here is equally applicable to incompressible and compressible seals, for conciseness only results pertaining to incompressible seals will be presented.

CLOSED-FORM SOLUTIONS TO GW/CEB CONTACT MODEL

At startup or shutdown seal faces start at contact or come into contact. Likewise, an excessive relative tilt between stator and rotor, as caused by transient dynamic responses, may also cause face contact. Chang et al. (1987) developed a plastic contact model (CEB) that supplemented the Greenwood and Williamson (1966) elastic contact model (GW). Notably, the CEB model contains approximations: (1) the shape of the contact area is not accurately captured, (2) the volume assumed to be conserved during plastic deformation is set arbitrarily, and (3) that outside this volume an asperity remains undeformed (although beneath the plastically deformed region the asperity is bound to deform also elastically). Since the transition from the elastic regime (GW) to the plastic regime (CEB) is abrupt, Zhao et al. (2000) proposed a mathematical (polynomial) template to allow a "smooth transition" between the two regimes. Because eventually any contact model accumulates statistically the contribution of all asperity contact points, the integration process tends to diminish the deviations between the various models (suggesting a dominance by the statistics rather than by the models). All aforementioned models apply to static conditions. In the absence of an elastoplastic dynamic contact model the GW/CEB model is chosen here, despite its aforementioned limitations.

The following analysis is not limited to seals, unless otherwise noted. The original CEB work calculated the various integrals numerically because of the perceived complexity confederated by the Gaussian distribution. To bypass such cumbersome numerical integrations the Gaussian distribution has commonly been replaced with simplified exponential distribution functions to allow for closed-form solutions (see GW (1966), Etsion and Front (1994), Polycarpou and Etsion (1999), Hess and Soom (1992, 1993), Liu et al. (2000)). This work is different: (1) the Gaussian distribution is not compromised, (2) the integration results are obtained mathematically for the plastic regime exactly, and (3) the mean value theorem is used to approximate the integrals for the elastic regime. This work adheres to the definitions and nomenclature of CEB (1987) and Etsion and Front (1996), and the reader is referred to that work. Therefore, in this section $\beta = \eta R \sigma$ (distinguished from face coning). Also here, η is the areal density of asperities, R is the asperity radius of curvature, K is maximum contact pressure factor, $h^* = h/\sigma$ is the dimensionless mean separation, σ is the standard deviation of surface heights, σ_s is the standard deviation of asperity heights, and y_s is the distance between the means of asperity and surface heights. The latter two normalized parameters are $\sigma_s^* = \sigma_s/\sigma$ and $y_s^* = y_s/\sigma$. Also the height of an asperity measured from the mean of asperity heights, z, is normalized, $z^* = z/\sigma$.

An "average"contact pressure is now defined by $p_c = F/A_n$ where F is the contact force and A_n is a nominal contact area. Then the elastic and plastic components are calculated, respectively, by

$$p_{ce} = \frac{4}{3}\beta(\frac{\sigma}{R})^{1/2}E \cdot I_e \qquad [1a]$$

$$p_{cp} = \beta\pi KH \cdot I_p \qquad [1b]$$

where

$$I_e = \int_a^{a_2} (z^* - a)^{3/2}\varphi^*(z^*)dz^* \qquad [2a]$$

$$I_p = \int_{a_2}^{\infty} 2(z^* - a_1)\varphi^*(z^*)dz^* \qquad [2b]$$

The integrals contain the following definitions: $a = h^* - y_s^*$; $a_1 = a + \omega_c^*/2$; $a_2 = a + \omega_c^*$; where the critical interference is $\omega_c^* = \sigma_s^*/\psi^2$, and ψ is the plasticity index as defined by GW (1966). The Gaussian distribution is given by

$$\varphi^*(z^*) = \frac{1}{\sqrt{2\pi}}(\frac{\sigma}{\sigma_s})exp[-0.5(\frac{\sigma}{\sigma_s})^2 z^{*2}] \qquad [3]$$

The Elastic Contact Model - Approximate Solution

In many applications $\psi^2 >> 1$ (as it is typically in mechanical seals). Since also $\sigma_s^* \approx 1$ then $\omega_c^* << 1$. This condition is not mathematically necessary, but it may improve upon the approximation.

The integrand in Eq. [2a], $f(z^*) = (z^* - a)^{3/2}\varphi^*(z^*)$, is continuous; hence, the mean value theorem can be used,

$$f(\xi) = \frac{1}{a_2 - a}\int_a^{a_2} f(z^*)dz^* \qquad [4]$$

where $f(\xi)$ is the mean value of $f(z^*)$ calculated at some $\xi \in [a, a_2]$. Noting that $a_2 - a = \omega_c^*$ in Eq. [4], and applying to the integral of Eq. [2a], gives

$$I_e = \int_a^{a_2} f(z^*)dz^* = f(\xi)\omega_c^* \qquad [5]$$

The compromise in the results depends only upon where ξ is selected. If the mean is assumed to prevail at the mid-range $\xi \equiv z^* = a + \omega_c^*/2 \equiv a_1$, it leads to an approximation of Eq. [2a]

$$I_e \approx (\frac{1}{2})^{3/2}\omega_c^{*5/2}\varphi^*(a_1) \qquad [6]$$

Substitution in Eq. [1a] yields

$$p_{ce} \approx \frac{\sqrt{2}}{3}\beta(\frac{\sigma}{R})^{1/2}E\omega_c^{*5/2}\varphi^*(a_1) \qquad [7a]$$

Although not used here, but for completeness, the elastic area of contact is also obtained. Using Eq. [42] in CEB (1987), and applying similarly the mean value theorem gives,

$$\frac{A_e}{A_n} = \pi\beta\int_a^{a_2} (z^* - a)\varphi^*(z^*)dz^*$$

$$\approx \pi\beta\frac{\omega_c^{*2}}{2}\varphi^*(a_1) \qquad [7b]$$

The Plastic Contact Model - Exact Solution

The integration of Eq. [2b] is carried out mathematically to yield exactly

$$I_p = \sqrt{\frac{2}{\pi}}\sigma_s^*exp[-\frac{1}{2}(\frac{a_2}{\sigma_s^*})^2] - a_1 erfc(\frac{a_2}{\sqrt{2}\sigma_s^*}) \qquad [8]$$

The complimentary error function, $erfc(\cdot)$, is calculated using either intrinsic functions, subroutine packages, or it can easily be hand-coded (Press, et al., 1994). Upon substitution of Eq. [8] in Eq. [1b] results in

$$p_{cp} = \beta\pi KH\{\sqrt{\frac{2}{\pi}}\sigma_s^*exp[-\frac{1}{2}(\frac{a_2}{\sigma_s^*})^2] - a_1 erfc(\frac{a_2}{\sqrt{2}\sigma_s^*})\} \qquad [9a]$$

The plastic area of contact is defined by Eq. [43] in CEB (1987). Hence, the exact solution is

$$\frac{A_p}{A_n} = \pi\beta \cdot I_p = \sqrt{2\pi}\beta\sigma_s^*exp[-\frac{1}{2}(\frac{a_2}{\sigma_s^*})^2] - \pi\beta a_1 erfc(\frac{a_2}{\sqrt{2}\sigma_s^*}) \qquad [9b]$$

Collecting the elastic and plastic contributions, the total average contact pressure over a nominal area A_n is

$$p_c = p_{ce} + p_{cp} \qquad [10]$$

It is emphasized that all results obtained here are derived in closed-form, so there is no overhead associated with their computation. Moreover, the Gaussian distribution is not approximated (as was done elsewhere) and particularly, the result in Eq. [9a] is exact. Since mechanical seals predominantly inherit large plasticity indexes, Eq. [9a] is dominant, and practically $p_c \approx p_{cp}$. Nevertheless, Eq. [10] is used for the force and moment balance, allowing seamless seal transition between contacting and noncontacting modes of operation. After face liftoff, or during noncontacting operation, h^* becomes sufficiently large ($h^* > 3$) to make this model mathematically moot.

FACE DEFORMATION

This work strictly adheres to the kinematical model developed by Green and Etsion (1985, and 1986). For conciseness the model will only be briefly described, while emphasis is placed upon new information that pertains to the current task. Figures 1 and 2 are taken from the aforementioned work to assist in model description.

The film thickness distribution is directly influenced by face deformation, which is caused by- thermally and mechanically
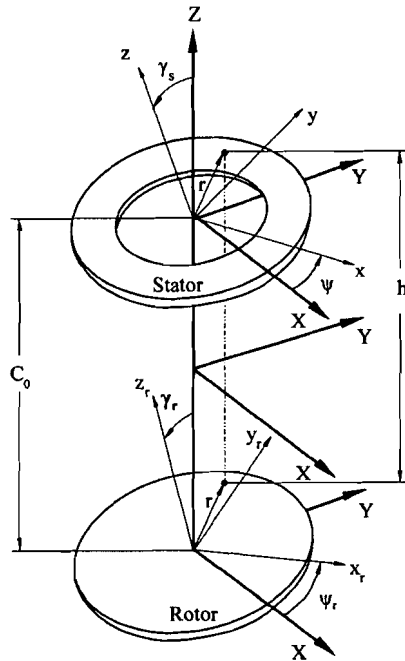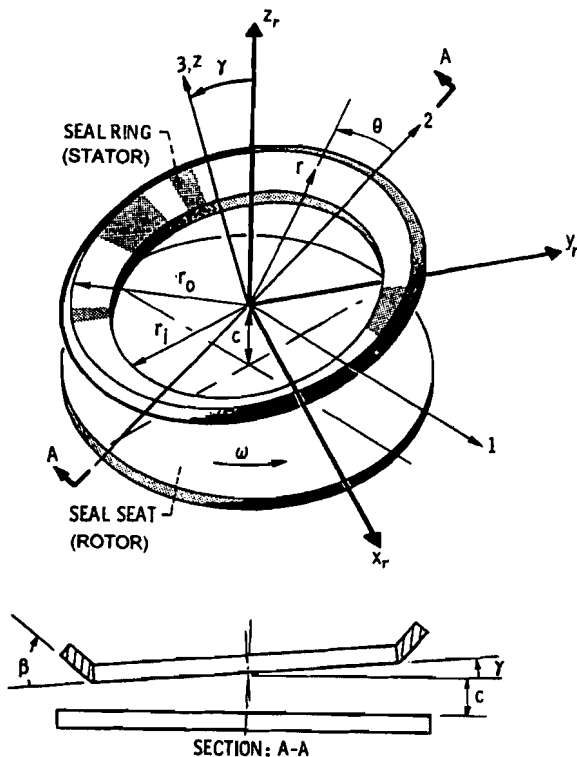
Fig. 1—Seal kinematical model.

Fig. 2—Relative position between stator and rotor.

induced effects. The thermal deformation is caused by viscous and frictional heating, where the mechanical deformation is caused by fluid pressure, centrifugal effects, and contact. These deformations can be calculated by a finite element structural analysis. This method, however, requires a large amount of computing time because the deformation calculations have to be repeated at every instant (see e.g., Parmar, 1992) due to the coupling between the

lubrication, heating, and the deformation processes. To bypass this time consuming calculation Taylor (1992), and then Ruan et al. (1997), devised an influence coefficient technique that was also used by Harp and Salant (1997). This technique assumes that the deformation is linearly dependent upon the external loadings. The approach also assumes that the deformations occur instantaneously as the loads are applied, or implicitly assumes quasi-static conditions. When mechanical loadings are of concern, indeed the seal structure reacts (deforms) without lag. However, when thermal loadings are of concern deformations lag behind. Specifically, consider viscous heating in a transient state: the temperature field in the seal elements is governed by the time dependent Fourier Equation. The deformation (face warping) then, as caused by the temperature gradients in the material, changes and evolves in time. Thus, a transient analysis must account for this time dependent warping as viscous heating and the film thickness are entangled. To implement time dependent spatial influence coefficients is a cumbersome process. Instead, a pragmatic approach is proposed here. First, only viscous heating is considered here, because experience shows that this is the dominant effect in face warping once thermal deformation takes place, which causes the frictional heating to vanish sharply (Parmar, 1992). However, if deemed necessary the treatment of frictional heating can easily be implemented using the same technique outlined here (this will be highlighted later). Second, similar to Parmar (1992), mechanically induced deformations are not included as they are typically much smaller than thermally induced deformations, but if deemed important their inclusion is trivial (Ruan et al., 1997).

Consider the time dependent Fourier Equation. Suppose that a solid is at a uniform reference temperature and a unit heat source is applied to the solid boundary. The temperature field would propagate in a monotonic fashion, and would exponentially change in time at any point in the solid (Özisik, 1993, Ch. 2). The spatial temperature gradient that is formed, coupled with the elastic governing equations, would in turn deform the boundary in a likewise monotonic fashion. Finite element codes are well suited to solve the thermal and the elastic problems seamlessly. That face warping is shown schematically in Fig. 3, where β represents axisymmetric and linear face coning (see Fig. 2). The axisymmetric linear shape may be assumed as a first approximation, but if the faces deform in some curved or wavy fashion, then other spatial shape functions can likewise be used because the solution of the time-dependent Fourier equation is separable in time and space (i.e., solved by separation of variables). Particularly, since the transient dynamic analysis herein is by definition non-axisymmetric it can easily accommodate non-axisymmetric deformations.

Instead of a unit source, the deformation is obtained at a reference value of the film thickness and speed, denoted as h_{ref} and ω_{ref} respectively, where β_{ref} is the asymptotic value of the deformation for these conditions. It seems that the warping behavior resembles a first order system response, in which case, since viscous heating and thus warping are proportional to ω^2/h (Ruan et al., 1997), a governing equation can be formed[1]:

---

[1] Equation [11] is similar to Eq. [6-132] in Szeri (1980) for a marching process. With knowledge of the boundary conditions and the deformation at one instant in time, one can compute the deformation at all later times.
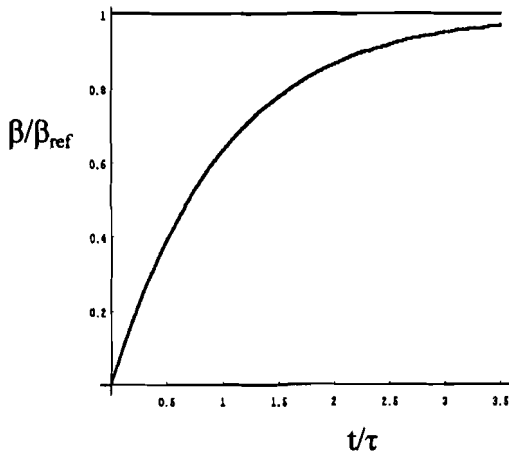
Fig. 3—Schematic of face deformation vs. time.

$$\tau\frac{d\beta}{dt} + \beta = \beta_{ref}[(\frac{h_{ref}}{h})(\frac{\omega}{\omega_{ref}})^2] \qquad [11]$$

Note that when $h=h_{ref}$ and $\omega=\omega_{ref}$ are applied at $t=0$, then Eq. [11] can be written as

$$\tau\frac{d\delta}{dt} + \delta = u(t) \qquad [12]$$

where $\delta=\beta/\beta_{ref}$ and $u(t)$ represents a unit step function. The solution of this equation is

$$\delta(t) = 1 - e^{-t/\tau} \qquad [13]$$

where τ is the time constant of the process. When $t/\tau=1$, δ achieves the value of 0.632, which allows the extraction of τ from the transient deformation results originating from the finite element solution (Fig. 3). The right hand side of Eq. [11] suggests that the larger the speed and the smaller the film thickness, the larger the deformation. However, $h=h(t)$ and $\omega=\omega(t)$, i.e., they are functions of time in a transient response. Hence, under these conditions Eq. [11] becomes

$$\tau\frac{d\delta}{dt} + \delta = f(t) \qquad [14]$$

where $f(t)=[h_{ref}/h(t)][\omega(t)/\omega_{ref}]^2$. [Note that if THD is accounted for (e.g., Pascovici and Etsion, 1992) and the viscosity becomes time dependent, then the right hand side of Eq. [11] and $f(t)$ can be augmented, i.e., multiplied by $\mu(t)/\mu_{ref}$, and the outlined procedure remains intact.] The general solution of Eq. [14] is (see Meirovitch, 2001)

$$\delta(t) = \varphi(t)\delta(0) + \int_0^t \frac{\varphi(t-\zeta)}{\tau}f(\zeta)d\zeta \qquad [15]$$

Hence, the deformation at any time is obtained by convolution of the forcing function $f(t)$ and a kernel solution $\varphi(t)/\tau$, where

$$\varphi(t) = L^{-1}[\frac{\tau}{s+\tau}] = e^{-t/\tau}$$

Here s is the Laplace variable, and L^{-1} is the inverse Laplace transform. The initial condition of the deformation is $\delta(0)$ (in a typical face flat seal this is zero, but any other initial value can be used). The solution of Eq. [14] is thus

$$\delta(t) = e^{-t/\tau}\delta(0) + \frac{e^{-t/\tau}}{\tau} * f(t) \qquad [16]$$

where the star product represents the convolution expressed in Eq. [15]. Clearly the deformation at any instant depends upon the entire deformation history, i.e., the process is hereditary. For this reason the quasi-static assumption used in other work may not be suitable to describe transient processes. There are two exceptions to this conclusion and they are the limiting cases of τ:

1. The time constant is very large $\tau \rightarrow \infty$. In this case $d\delta/dt\rightarrow0$ and the solution is simply $\delta(t)=\delta(0)$, i.e., the deformation is equal to the initial value and remains constant throughout. This may represent the case when viscous heating has a negligible effect upon the deformation.

2. The time constant is very small $\tau \rightarrow 0$. In this case (see Eq. [14]) $\delta=f(t)$, i.e., the deformation occurs instantaneously. In this situation the quasi-static solution may be justified. However, the consequences of letting $\tau \rightarrow 0$ may be erroneous because if the system is brought instantaneously to stand still (i.e., if the heat generation has become immediately nil), the seal faces may still be warped, and leakage would continue until the faces cool off completely. Only careful examination of τ compared to other time scales in the problem (e.g., in dynamics, the inverse of the eigenvalues and/or shaft speed) will reveal whether letting $\tau \rightarrow 0$ is justified. [For mechanically induced warping, by definition, $\tau=0$.]

Clearly the solution presented above can equally be applied to asperity friction, if so desired. The frictional heating generated would add to the viscous heating, and face deformation would only be expedited. Once pressure builds up in a radially converging gap, faces lift off rapidly (see also Parmar, 1992, and the results that follow) negating the frictional heating effects and leaving viscous heating to dominate. Once noncontacting operation has been established frictional heating is moot along with the contact forces.

While the solution given in Eq. [16] is viable, the numerical implementation of convolution coupled with dynamics, although possible, is more cumbersome than the technique presented subsequently.

TRANSIENT OPERATION CONDITIONS

To represent time-varying conditions (startup, running, and shutdown) the following generic function is assumed:

$$f = 0 \qquad\qquad t < 0, t > t_3$$

$$f = V\frac{t}{t_1} \qquad\qquad 0 \le t \le t_1 \qquad [17]$$

$$f = V \qquad\qquad t_1 \le t \le t_2$$

$$f = V(1 - \frac{t - t_2}{t_3 - t_2}) \qquad t_2 \le t \le t_3$$

where V is a desired steady-state value representing generically the rotor angular velocity, $\dot\psi_r = \omega$, or seal inner or outer pressures, p_i, or p_o, respectively. Judicious use of t_1, t_2, and t_3, such that $0 \le t_1 \le t_2 \le t_3$, can bring about function combinations of constant, ramp-up-and-down, step, etc. It is not necessary that the various values of t_i be the same for speed and pressure.

SIMULTANEOUS SOLUTION OF TRANSIENT DYNAMICS

The analysis herein pertains to a mechanical seal having a flexibly mounted stator configuration. The kinematical model and analysis strictly conform in essence and nomenclature with Green and Etsion (1985, 1986). That work in the current analysis can be regarded as having $\tau \to \infty$, and $t_1 = 0$, $t_2 = t_3 \to \infty$. Because of this conformity the kinematical model is not repeated. Only essential and new information is added here. Note particularly the new definition of rotor precession, $\dot\psi_r$, which will be discussed below.

The rotating seal seat (rotor) is rigidly mounted to the rotating shaft. The flexibly supported seal ring (stator) is attempting to track the misaligned rotor (see Fig. 1). The rotor misalignment is represented by a tilt γ_r measured between the out-normal to its plane and the axis of shaft rotation. Similarly, the stator may have, prior to final attachment to the rotor, an initial misalignment, γ_{si}, measured with respect to the axis of shaft rotation. At rest, and with zero pressure differential, the stator is pressed against the rotor by supporting springs. This forces the stator into the same tilt as that of the rotor where both rest on asperity contact. During operation, however, the mating faces separate and the stator detaches from the rotor to assume its own tilt, γ_s. This tilt is a result of the combined effects of both γ_r and γ_{si}. The tilt angles γ_{si}, γ_r, and γ_s are all very small, typically less than one milliradian and, therefore, they can be treated as vectors. Since γ_{si} is fixed in space and γ_r is rotating at the shaft speed ω, the resultant vector γ_s will possess a time-varying precession (whirl) speed, $\dot\psi$. Green and Etsion (1985), expressed the vector γ_s as follows:

$$\vec\gamma_s = \vec\gamma_{sI} + \vec\gamma_{sr} \qquad [18]$$

where $\vec\gamma_{sI}$ is the response to $\vec\gamma_{si}$ alone and is fixed in space, while $\vec\gamma_{sr}$ is the response to $\vec\gamma_r$ alone and thus is whirling at the shaft speed. The relative misalignment between the stator and rotor, γ, is also a rotating vector, given by the vector subtraction and its magnitude:

$$\vec\gamma = \vec\gamma_s - \vec\gamma_r ;$$

$$|\gamma| = [\gamma_s^2 + \gamma_r^2 - 2\gamma_s\gamma_r cos(\psi - \psi_r)]^{1/2} ; \qquad [19]$$

$$\psi_r(t) = \int_0^t \dot\psi_r dt$$

where $\psi_r(t)$ is the time varying rotor precession angle and is obtained by the analytical integration of Eq. [19]. Figure 2 shows the relative position between the seal components. The tilt vector γ_o is the relative misalignment γ in the special case when $\gamma_{sI} = 0$, and by using Eqs. [18]-[19] gives:

$$\vec\gamma_o = \vec\gamma_{sr} - \vec\gamma_r \qquad [20]$$

The support moments and force are

$$M_{sx} = K_s(\gamma_{si}cos\psi - \gamma_s) - D_s\dot\gamma_s \qquad [21a]$$

$$M_{sy} = -K_s\gamma_{si}sin\psi - D_s\dot\psi\gamma_s \qquad [21b]$$

$$F_{sZ} = -K_{sZ}Z - D_{sZ}\dot Z \qquad [21c]$$

where K_{sZ} and D_{sZ} are, respectively, the axial stiffness and damping coefficients of the support. Note here that the term γ_{si} in Eq. [21] is the initial stator misalignment that produces an inertial forcing function. This is the result of manufacturing and assembly imperfections (tolerances), or the action of gravity. For conciseness it is assumed in this work (without loss of generality) that $\gamma_{si} = 0$.

The closing force is due to hydraulic pressure and spring preset

$$F_{cls} = F_{hyd} + F_{spr}$$

$$F_{hyd} = \pi[(r_o^2 - r_b^2)p_o + (r_b^2 - r_i^2)p_i]$$

$$= \pi(r_o^2 - r_i^2)(B_o p_o + B_i p_i) \qquad [22]$$

$$B_o = \frac{r_o^2 - r_b^2}{r_o^2 - r_i^2} ; \quad B_i = \frac{r_b^2 - r_i^2}{r_o^2 - r_i^2} ;$$

$$B_o + B_i = 1$$

where r_i, r_o, r_b are the seal inner, outer, and balance radii, respectively. B_o and B_i are area ratios, one of which is designated as the balance ratio, B: if $p_o > p_i$ then $B = B_o$, if $p_i > p_o$ then $B = B_i$.

The flow is governed by the incompressible Reynolds equation assuming isoviscous conditions (see comment following Eq. [14] concerning time-dependent viscosity). Hence,

$$\vec\nabla \cdot [\frac{h^3\vec\nabla p}{12\mu} - \frac{1}{2}\omega r h\vec{i}_\theta] = \frac{\partial h}{\partial t} \qquad [23]$$

where the operator $\vec\nabla$ is presumed to be in cylindrical coordinates. Since the intent here is to solve a transient behavior from contact to separation, it seems as if the flow factors such as those obtained by Patir and Cheng (1978, 1979) need to be included. However, as will be shown later, even the heavily overbalanced seals examined here do not have a ratio h/σ less than three. Consequently the flow factors asymptotically approach the value of unity and, therefore, can be ignored. The solution of Eq. [23] for the pressure is presented in closed-form in Green and Etsion (1985, 1986), and is not

TABLE 1—REFERENCE CASE $(\tau = 2\ s,\ B = 0.75)$			
$r_i = 0.0355\ m$	$r_o = r_g = 0.0408\ m$	$\mu = 1.2 \cdot 10^{-3}\ Pa\ s$	$\gamma_r = 10^{-3}\ rad$
$K_{Zs} = 5 \cdot 10^5\ N/m$	$D_{Zs} = 300\ N\ s/m$	$F_{spring} = 20\ N$	$m = 1\ kg$
$\beta_{ref} = 5 \cdot 10^{-6}\ rad$	$h_{ref} = 0.3 \cdot 10^{-6}\ m$	$\omega_{ref} = 500\ rad/s$	$\beta(0) = 0$
$H = 1\ GPa$	$R = 1.7 \cdot 10^{-6}\ m$	$K = 0.6$	$C_o = 10^{-6}\ m$
$E = 24.07\ GPa$	$\sigma = 10^{-7}\ m$	$\psi = 6.167$	$\eta = 4.16 \cdot 10^{11}$
TRANSIENT PROPERTIES. $p_i = 100\ kPa = const$ [SEE EQ. [17]]			
Steady-state value between t_1 and t_2	t_1	t_2	t_3
$p_o = 500\ kPa$	3 s	6 s	9 s
$\omega = 1500\ rad/s$	3 s	6 s	9 s

repeated. The only compromise imbedded in the solution is that of the "narrow seal approximation (Etsion, 1980)," which is well justified for most mechanical seals.

Clearly the solution for p is dependent upon h and $\partial h/\partial t$ (see Eq. [23]). Using Fig. 2, and noting that $C = C_o + Z$, where C_o is the designed centerline clearance, leads to the local film thickness

$$h = C_o + Z + \gamma r cos(\theta) + \beta(r - r_i) \qquad [24]$$

where β is the time-dependent coning angle (see Eq. [11]), and γ is the relative misalignment. The latter is calculated by using Eq. [19]. The stator degrees of freedom are the axial displacement, Z, the nutation, γ_s, and the precession, ψ. At every instant of time the interface induces tilting moments and an axial force that are obtained by integrating the fluid film pressure, p, combined with the contact pressure, p_c (from Eq. [10]), over the sealing dam area:

$$M_{fx} = \int_0^{2\pi} \int_{r_i}^{r_o} (p + p_c) r^2 sin(\theta - \psi) dr d\theta \qquad [25a]$$

$$M_{fy} = -\int_0^{2\pi} \int_{r_i}^{r_o} (p + p_c) r^2 cos(\theta - \psi) dr d\theta \qquad [25b]$$

$$F_{fz} = \int_0^{2\pi} \int_{r_i}^{r_o} (p + p_c) r dr d\theta \qquad [25c]$$

A numerical integration is used because intermittent contact and/or cavitation make the problem nonlinear. Cavitation (a condition more likely to happen in low-pressure and high-speed seals, but unlikely otherwise) is handled here using the half-Sommerfeld boundary condition. Since Z, γ_s, and ψ are time dependent then h, p, M_{fx}, M_{fy}, and F_{fz} are time dependent as well. The equations of motion (Green and Etsion, 1985, 1986) as formulated by Green and Barnsby (2001) are cast in a state space form, including now the time-dependent face coning of Eq. [11],

$$\frac{\partial}{\partial t}\begin{Bmatrix} \dot{Z} \\ Z \\ \dot{\gamma_s} \\ \gamma_s \\ \dot{\psi} \\ \psi \\ \beta \end{Bmatrix} = \begin{Bmatrix} (F_{sZ} + F_{fZ} - F_{cls})/m \\ \dot{Z} \\ (M_{sx} + M_{fx})/I + \dot{\psi}^2 \gamma_s \\ \dot{\gamma_s} \\ [(M_{sy} + M_{fy})/I - 2\dot{\psi}\dot{\gamma_s}]/\gamma_s \\ \dot{\psi} \\ \{\beta_{ref}[(h_{ref}/h)(\dot{\psi}_r/\omega_{ref})^2] - \beta\}/\tau \end{Bmatrix} \qquad [26]$$

These are subject to the initial conditions $Z(0) = -0.65C_o, \gamma_s(0) = \gamma_r, \dot{Z}(0) = \dot{\gamma_s}(0) = \psi(0) = \dot{\psi}(0) = \beta(0) = 0$. Note that the lubrication problem, dynamics, and face warping are all coupled. This nonlinear set of seven equations is integrated in time by efficient multistep ordinary differential equation solvers (Shampine, 1994). The solution gives a simultaneous dynamic simulation for the transient response of the seal including face deformation caused by viscous heating.

PARAMETRIC INVESTIGATION

A typical reference case is selected (see Table 1). For those h_{ref} and ω_{ref} specified, a thermal time constant, τ, and a reference (steady-state) coning, β_{ref} have been extracted from transient coning results calculated by an FEA code (see discussion following Eq. [13]). [The value of $\tau = 2\ s$ is by and large consistent with that of $4\ s$ reported by Parmar (1992) to reach steady-state coning]. In the present analysis the seal is set into motion from rest at easy contact $(h_{min}/\sigma = 0.35C_o/\sigma = 3.5)$. According to Eq. [17] the speed, $\dot{\psi}_r$, and pressure drop, $p_o - p_i$, are simultaneously ramped up to their respective maximums, held constant at steady-state values, and then ramped down to zero (the inner pressure is held constant). In this analysis two effects will be examined.

Balance Ratio Effects

Upper and lower balance ratios of 0.65 and 0.85 are compared against the reference value of 0.75, while the thermal time constant is held fixed at $2\ s$. The transient results are shown as a function of normalized time, $\omega t/2\pi$, in Fig. 4(a) for the normalized kinematical variables, and in Fig. 4(b) for the normalized coning and flow rate (see Nomenclature for normalization). It is seen that in all cases an initial transient occurs as speed, $\dot{\psi}_r$, and pressure difference, $p_o - p_i$, develop, i.e., when the balance ratio becomes
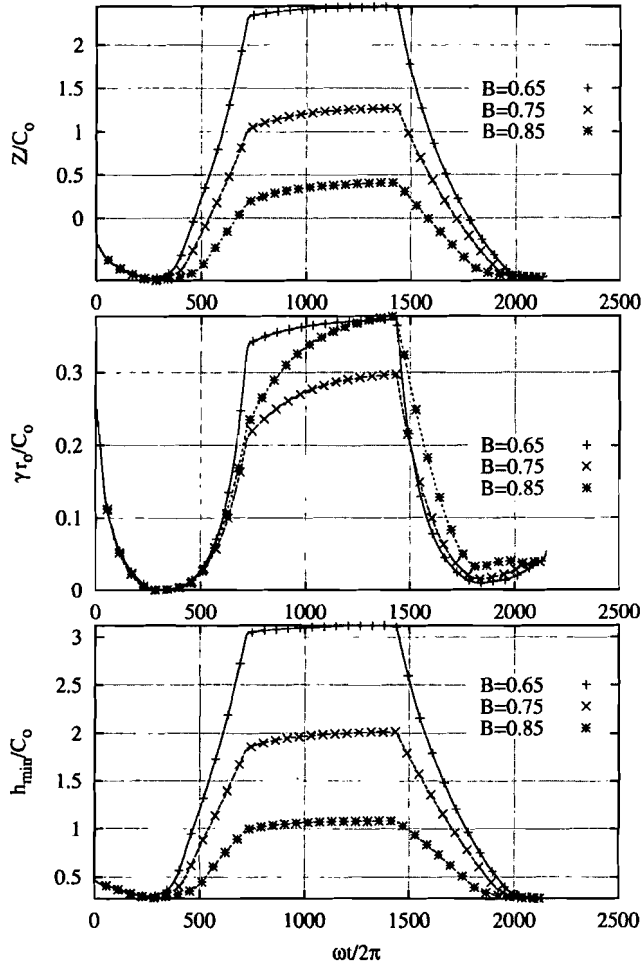
Fig. 4(a)—Balance ratio effects upon transient response (τ = 2 s).

Fig. 4(b)—Balance ratio effects upon coning and flow (τ = 2 s).

meaningful. Following that the seal starts and returns to contact exactly at or close to $\gamma = 0$, and $h_{min}/C_o = 0.3$. Since here $\sigma = 0.1$ μm and $C_o = 1$ μm, then $\lambda = h_{min}/\sigma = 3$ validating that flow factors (Patir and Cheng, 1978) are moot in this application even at contact.

The combination of thermal deformation (i.e., coning) and an evolving pressure drop induce a hydrostatic opening force that separates the faces from contact at rest to a noncontacting mode of operation. Hence, except for very short durations at startup or shutdown, viscous shear remains the only heating source. As can be seen in Fig. 4(b) the coning is time varying, starting at the initial value of zero (i.e., flat faces at rest and in contact) to a maximum, then upon shutdown as speed decreases, the faces cool off and the coning decreases. Nevertheless there remains some coning even at the end of the cycle because the time constant prevents an immediate reaction to zero heat generation. The flow, which increases with increased coning and pressure drop, goes down to zero even though there is some coning left. This is because at the end of the cycle the pressure drop also goes to zero. However if the pressure in the seal chamber had still been elevated, flow would have continued even at complete shutdown (this case will be demonstrated subsequently).

The effect of the balance ratio is almost intuitive: the larger the balance ratio the smaller the dynamic response, the larger the heat
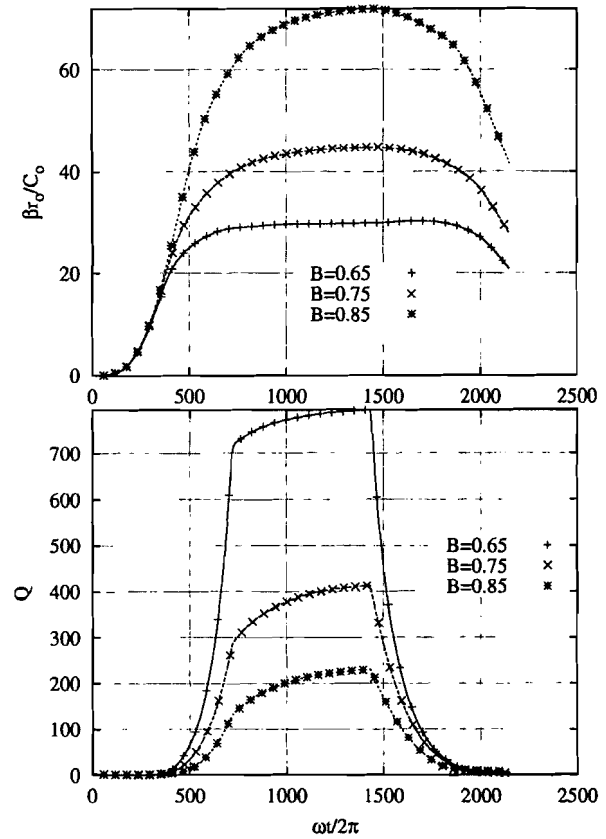
generation, the larger the coning, the smaller the leakage. (While wear is not part of the model, it is likely that also wear increases with the balance ratio.) There is one exception though: it is seen from Fig 4(a) that at the intermediate (i.e., reference) value of 0.75, the relative tilt is smaller than 0.65 or 0.85. This is the result of a smaller angular transmissibility (see Green and Etsion, 1985). Also, the decrease of the balance ratio from 0.85 to 0.65 in steps of 0.10, approximately doubles the flow rate at each step. It can also be seen that the thermal time constant is delaying the dynamic response of the seal, as discussed in the introduction. This effect is now further investigated.

Thermal Time Constant Effect

In this section the balance ratio is held constant at 0.75, while letting τ take on values of 0, 2, and 4 s. In addition, for the reference condition the outer pressure, p_o, is ramped up with speed as previously, but upon shut down the pressure remains at its maximum in order to simulate a condition of elevated pressure in the seal chamber even during shutdown. The dynamic response, deformation, and flow are shown in Fig. 5. It is obvious that when $\tau = 0$ the dynamic response is in phase with the deformation, showing a symmetric behavior having a constant steady-state value between startup and shutdown. At $\tau = 2$ s the deformation (coning) is delayed, and with it the system transient response is delayed until the steady-state value is reached, after which the system goes through a shutdown process. However, at $\tau = 4$ s the
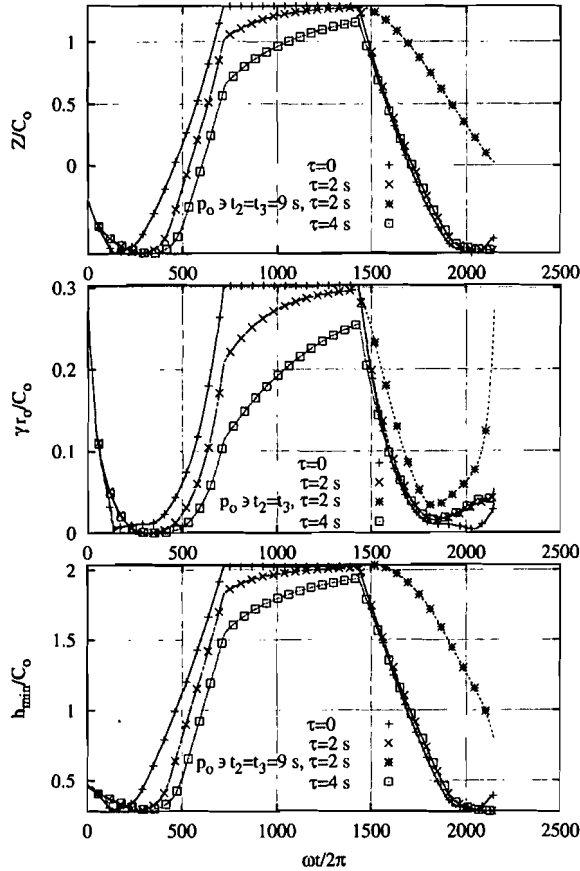
Fig. 5(a)—Thermal time constant effects upon the transient response (B = 0.75).

Fig. 5(b)—Time constant effects upon coning and flow (B = 0.75).

delay prevents the system from reaching the steady-state value before the seal shuts down. During the shutdown process the seal behavior is very similar in these three cases as the pressure drop decreases with speed (and with it the viscous heating).

It is interesting to note that when the outer pressure in the seal chamber remains elevated at shut down, $p_o = 500$ MPa, and letting $t_2 \equiv t_3 = 9\,s$, the seal at the end of the cycle ends up at a static balance where $Z/C_o = 0$, $\gamma r_o/C_o = 0.275$, and $h_{min}/C_o = 0.78$. That is, the seal faces remain open where the combination of elevated hydrostatic pressure drop and coning generate flow even at standstill (see Fig. 5(b)). Then the coning drops off more rapidly as the flow cools off the faces. The total volumetric flow is the integral of Q in time, i.e., it is the area contained under the curve of Fig. 5(b). It is obvious that such a behavior adds considerably to flow escaping the seal even after shut down. It is concluded that the thermal time constant has a significant role during startups and shutdowns and in transients subject to similar time scales.

The CPU execution time is typically of the order of one minute on a 866 MHz PC for each of the aforementioned numerical examples.

SEPARATION SPEED OF CONTACTING SEALS

The computer code presented here has demonstrated its capability to seamlessly simulate the transition of seals going from contacting to noncontacting mode of operation, and vice versa.
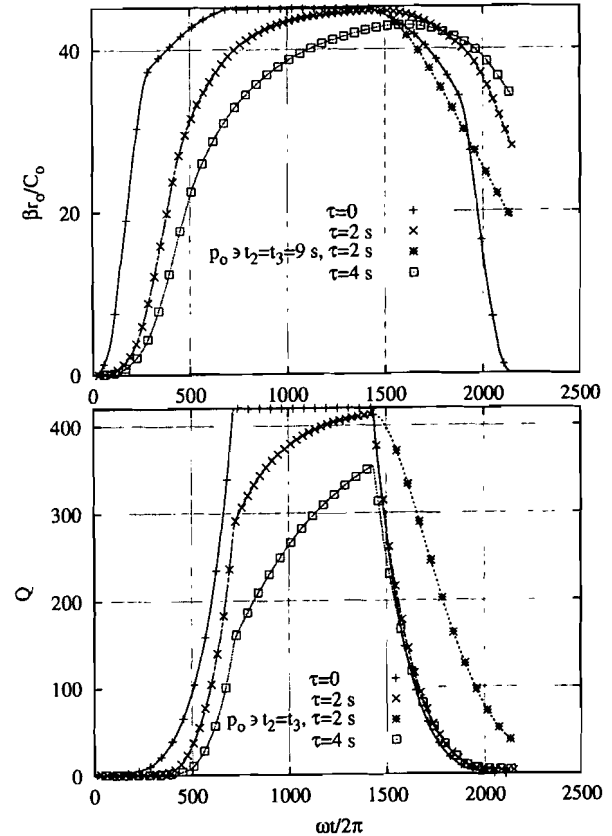
The works by Green (1990), and Green and Bair (1991) presented a closed-form solution for the separation speed of contacting seals. It is interesting to verify the current numerical simulation with the said work predictions. However, to achieve a closed-form solution, some simplifying assumptions had to be made. To comply with the conditions of the previous work it is assumed now that the pressure drop is nil, $\tau \rightarrow \infty$, and the rotor speed, $\dot{\psi}_r$, is linearly ramped up from zero to an arbitrarily "high target speed" of $\omega = 10^5\ rad/s$ at a rate of $\ddot{\psi}_r = 10^4\ rad/s^2$ (all other conditions in the base case of Table 1 remain unchanged). The results of the simulation for the kinematical variables are shown in Fig. 6 where the inset magnifies the neighborhood of separation. It can be seen that perfect contacting state prevails until the vicinity of $(\omega t/2\pi) = 1870$, beyond which the seal sharply opens up axially and angularly. A quick calculation using Eq. [17] reveals that at that instant the shaft speed is $\dot{\psi}_r = 1175\ rad/s$. This value is close to the separation speed of $1131\ rad/s$ predicted by the closed-form analysis of Green and Bair, 1991 (yielding a 4 percent difference). The aforementioned work assumed perfectly rigid surfaces, while here the analysis uses a finite interface stiffness (the GW/CEB contact model) which allows the faces to remain in contact a bit longer. It can be reasonably stated that the current numerical analysis is confirmed analytically. Of course, for realistic seals where the said idealization is not feasible the current numerical formulation remains the only viable design tool. The CPU execution time for this example is approximately two minutes.
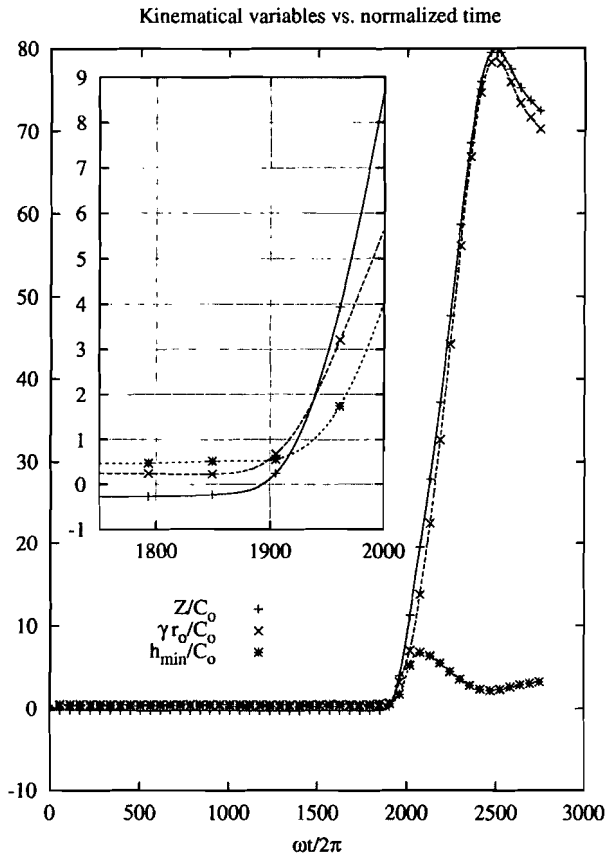
Kinematical variables vs. normalized time

Fig. 6—Separation speed of a contacting seal.

CONCLUSIONS

A transient dynamic analysis which includes time-dependent thermal deformation of the faces is presented. The proposed model shows that the thermal face deformation is hereditary by virtue of a finite thermal time constant. Instead of using a numerical convolution to capture the lag between cause and effect, the deformation model easily fits into a state-space form that already contains the dynamic equations of motion. These are integrated simultaneously by efficient multistep techniques. The current formulation circumvents the formidable task of a transient dynamic analysis coupled with a time dependent finite element analysis for the heat transfer and face deformations. The current formulation also includes a new closed-form solution for the mechanics of asperity contact, which allows a seamless dynamic simulation of real seals as they transition from contacting to noncontacting modes of operation, and vice versa.

The results show that thermally induced coning combined with a hydrostatic pressure drop lifts the faces off even at a fairly high balance ratio. After lift-off (and in the absence of stator initial misalignment) the stator synchronously tracks the rotor in time-delayed noncontacting mode of operation. A time lag takes place between the initiation of rotor rotation, heating, and lift-off. It is shown that a real seal can continue to leak even after shutdown when the pressure drop remains elevated because of residual coning in the faces that cool off gradually. The computer code is verified against a closed-form solution that predicts the separation

speed of contacting seals where the numerical simulation yields a less conservative (higher) critical speed because of interface compliance. Although the examples solved here pertain to incompressible fluids, the analysis can equally be applied to compressible seals; however, viscous heating effects would likely be smaller because of lower gas viscosity, but instead dry face friction may become dominant to generate a similar deformation pattern and dynamic behavior.

REFERENCES

(1) Chang, W. R., Etsion, I. and Bogy, D. B., (1987), "An Elastic-Plastic Model for the Contact of Roughness Surface," ASME Jour. of Trib., 109, pp 257-263.

(2) Doust, T. G. and Parmar, A., (1986), "Experimental and Theoretical Study of Pressure and Thermal Distortions in Mechanical Seal," ASLE Trans., 29, 2, pp 151-159.

(3) Etsion, I. and Front, I., (1994), "Model for Static Sealing Performance of End Face Seals," Trib. Trans., 37, 1, pp 111-119.

(4) Green, I. and Barnsby, R. M., (2001), "A Simultaneous Numerical Solution for the Lubrication and Dynamic Stability of Noncontacting Gas Face Seals," ASME Trans., Jour. of Trib., 123, 2, pp 388-394.

(5) Green, I. and Etsion, I., (1985), "Stability Threshold and Steady-State Response of Noncontacting Coned-Face Seals," ASLE Trans., 28, 4, pp 449-460.

(6) Green, I. and Etsion, I., (1986), "Nonlinear Dynamic Analysis of Noncontacting Coned-Face Mechanical Seals," ASLE Trans., 29, 3, pp 383-393.

(7) Green, I., (1990), "Separation Speed of Undamped Metal Bellows Contacting Mechanical Seals," Trib. Trans., 33, 2, pp 171-178.

(8) Green, I. and Bair, S., (1991), "Dynamic Response to Axial Oscillation and Rotating Seat Runout of Contacting Mechanical Face Seals," Trib. Trans., 34, 2, pp 169-176.

(9) Greenwood, J. A. and Williamson, J. B. P., (1966), "Contact of Nominally Flat Surfaces," in Proc. of Roy. Soc. London, A, 295, pp 300-319.

(10) Etsion, I., (1980), "Accuracy of the Narrow Seal Approximation Analyzing Radial Face Seals," ASLE Trans., 23, 2, pp 208-216.

(11) Hess, D. P. and Soom, A., (1992), "Normal and Angular Motions at Rough Planar Contacts During Sliding with Friction," ASME, Jour. of Trib., 114, 3, pp 567-578.

(12) Hess, D. P. and Soom, A., (1993), "Effects of Relative Angular Motions on Friction at Rough Planar Contacts," ASME, Jour. of Trib., 115, 1, pp 96-101.

(13) Harp, S. R. and Salant, R. F., (1997), "Analysis of Mechanical Seal Behavior During Transient Operation," in Proc. ASME of the 1997 Joint ASME/STLE/IMechE World Tribology Conference, London UK.

(14) Liu, Z., Neville, A. and Reuben, R. L., (2000), "Analytical Solution for Elastic and Elastic-plastic Contact Models," Trib. Trans., 43, 4, pp 627-634.

(15) Meirovitch, L., (2001), Fundamentals of Vibrations, McGraw-Hill, Boston.

(16) Özisik, M. N., (1993), Heat Conduction, 2nd ed., John Wiley, New York.

(17) Parmar, A., (1992), "Thermal Cycling in Mechanical Seals - Causes, Prediction, Prevention," in Proc. BHRA of the 13th Int. Conf. on Fluid Sealing, pp 507-526.

(18) Pascovici, M. D. and Etsion, I., (1992), "Thermo-hydrodynamic Analysis of a Mechanical Face Seal," ASME, Jour. of Trib., 114, 4, pp 639-645.

(19) Patir, N. and Cheng, H. S., (1978), "An Average Flow Model for Determining Effects of Three- Dimensional Roughness on Partial Hydrodynamic Lubrication," ASME Jour. of Lubr. Tech., 100, 1, pp 12-17.

(20) Patir, N. and Cheng, H. S., (1979), "Application of Average Flow Model to Lubrication Between Rough Sliding Surfaces," ASME Jour. of Lubr. Tech., 101, pp 220-230.

(21) Polycarpou, A. A. and Etsion, I., (1999), "Analytical Approximations in Modeling Contacting Rough Surfaces," ASME, Jour. of Trib., 121, 2, pp 234-239.

(22) Press, W. H., Teukolsky, S. A., Vetterling, W. T. and Flannery, B. P., (1994), Numerical Recipes in FORTRAN: The Art of Scientific Computing, 2nd ed., Cambridge University Press.

(23) Ruan, B., Salant, R. and Green, I., (1997), "A Mixed Lubrication Model of Liquid/Gas Mechanical Face Seals," Trib. Trans., 40, 4, pp 647-657

(24) Shampine, L. F., (1994), Numerical Solution of Ordinary Differential Equations, Chapman and Hall, New York.

(25) Szeri, A. Z., (1980), Tribology: Friction, Lubrication, and Wear, Hemisphere, New York.

(26) Taylor, T., (1992), "Finite Element Solution of Gas Lubricated Mechanical Face Seal," MS Thesis, Georgia Institute of Technology.

(27) Zhao, Y., Maietta, D. M. and Chang, L., (2000), "An Asperity Microcontact Model Incorporating the Transition from Elastic Deformation to Fully Plastic Flow," ASME Jour. of Trib., 122, 1, pp 86-93.